buildings

MDPI

Article

Investigation of Ventilation Systems to Improve Air Quality in the Occupied Zone in Office Buildings

Szabolcs Szekeres, Attila Kostyák, Ferenc Szodrai and Imre Csáky *

Department of Building Services and Building Engineering, Faculty of Engineering, University of Debrecen, Ótemető str. 2-4, 4028 Debrecen, Hungary; szekeres@eng.unideb.hu (S.S.); kostyak.attila@eng.unideb.hu (A.K.); szodrai@eng.unideb.hu (F.S.)

* Correspondence: imrecsaky@eng.unideb.hu; Tel.: +36-52-415-155 (ext. 77772)

Abstract: As a result of COVID-19, many office buildings around the world have downsized their employees, but the comfort parameters in the building had to be kept. The facilities operation rearranged the workstations to keep physical distance and placed plexiglass sheets on the desks for physical protection. A series of measurements have been carried out with workstation set-ups to examine the fresh air rate in the occupied zone. The effect of plexiglass sheets placed on the desks was also examined to see how it changes the airflow pattern in the occupied zone. As the sheets act as a barrier, the *primary air* does not reach the occupied zone, therefore, the fresh air rate is less. To modify the properties of the ceiling diffusers a new air-ventilation service element was developed. This attachment allows modifying the properties of the ceiling diffusers. Simulations were made at the relevant zones to validate the measurements. Based on design software, the fresh air ratio for a standard ceiling swirl diffuser is 2.46 v% (volume percentage). A numerical model was used to show the fresh air ratio with the system elements for the two different table arrangements, which were 18.3 v% and 21.4 v%, respectively.

Keywords: indoor environments; induction rate; air velocity; draught; building occupants; workstation

Citation: Szekeres, S.; Kostyák, A.; Szodrai, F.; Csáky, I. Investigation of Ventilation Systems to Improve Air Quality in the Occupied Zone in Office Buildings. *Buildings* **2022**, *12*, 493. https://doi.org/10.3390/buildings12040493

Academic Editor: Ju-Hyeong Park

Received: 9 March 2022
Accepted: 13 April 2022
Published: 15 April 2022

1. Introduction

In the past couple of years, because of COVID-19, many office buildings around the world have downsized their staff, but the comfort parameters in the building had to be kept, therefore, the energy consumption remained similar. The final energy consumption by buildings reaches 39% of the total energy consumption in the EU and that includes the energy consumption by the HVAC systems [1]. This is significant as it reaches 50% of building consumption [2]. Therefore, we must strive to keep energy consumption by ventilation as low as possible.

The indoor air quality in the occupied zone became an important topic due to SARS-CoV-2 virus infection. The indoor air quality is affected by various factors, such as the fresh air ratio and the concentration of airborne pollutants. The general suggestion of the World Health Organization (WHO), the American Society of Heating, Refrigerating and Air conditioning Engineers (ASHRAE), and the Federation of European Heating, Ventilation, and Air Conditioning Associations (REHVA) to reduce the level of contamination of, for example, viruses and bacteria is to improve the air quality in the occupied zone by increasing the level of ventilation [3–5]. This generates higher energy consumption [6] and may affect the occupants' comfort as well. Natural ventilation has the advantage of energy efficiency but depends on the temperature difference between the internal and external air, and the position and size of the openings, therefore, it is difficult to regulate the ventilated amount of fresh air. Hence, in high comfort office buildings, mechanical ventilation is used to ensure the expected conditions. Other suggestions are physical distancing, protection, and barriers (plexiglass) between occupants. The barriers affect the airflow pattern in

the occupied zone hence the current ventilation system may not provide sufficient fresh air rate and that influences the air quality and the comfort factors. Occupants' comfort in buildings can be affected by several factors, such as noise, ergonomics, personal factors, health and wellbeing, indoor air quality, air temperature, air velocity, draughts, etc. Ventilation in buildings can be responsible for more than one of these factors. In office buildings, different ventilation modes are used, such as natural, mechanical ventilation, or both (natural or/and mechanical), which were examined in several articles [7,8]. Nguyen et al. analyzed the thermal comfort in Southeast Asia by the econometric method and presented the significance of air velocity in the occupied zone in buildings with natural ventilation [9]. Damiati et al. presented the comfort operative temperature in a tropical climate zone, and analyzed mean air velocity in thirteen office buildings that used natural, mechanical ventilation, or both. Based on the air movement vote of the occupants, the ideal mean air velocity ranged between 0.05 to 0.22 ms^{-1} which was considered in this study [10]. The previous case studies focused on the thermal comfort in the occupied zone but did not consider indoor air quality. The level of CO_2 is frequently examined in human bio-effluence studies as it gives valuable information about all other contamination associated with human bio-effluence [11–14].

In this paper, the measurements focused on different comfort factors (air temperature, air velocity, draughts), and air quality factors (fresh air rate) as these affect the working environment [15–17] created by mechanical ventilation. Diffusers are important elements in the mechanical ventilation mode as they can influence different comfort parameters. During the investigation, different diffusers were analyzed around different office desk layouts (office islands) with and without plexiglass barriers. The induction rate (the amount of mixing caused by the airflow entering the occupied zone can be characterized by the induction rate) was examined with a simulation model, which was validated with several measurements. A numerical analysis model was built similarly as in the studies where comfort factors were evaluated under different ventilation conditions [18] and CO distribution was examined [19]. During this study, the effect of different diffusers on the airflow pattern was analyzed in a laboratory environment. This study also aimed to increase the fresh air rate in the occupied zone without having to increase the energy consumption of the HVAC system and to achieve it on existing systems without any major alterations.

2. Experimental Methodology

2.1. Office Workstations

SARS-CoV-2, influenzas and other viruses are highly transmissible. These can be transmitted by inhalation of aerosols in which the virus can be found, hence mixing the air in the occupied zone is not favorable.

As shown in Figure 1 physical distance can be considered effective as the large respiratory droplets settling by gravity within this distance (1.5 m) will not reach the other person.

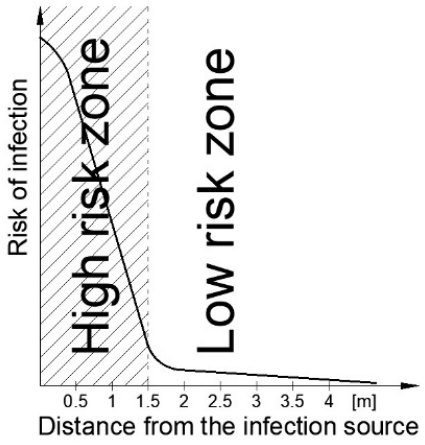

Figure 1. Relationship between infection risk and physical distancing [20].

Most office spaces are equipped with mixed ventilation, which leads to higher contamination concentration in the occupied zone. Research has been made to find typical workstation set-ups where physical distance can be kept, then two different set-ups were chosen from the popular ones suitable for four sitting persons as shown in Figure 2 [21].

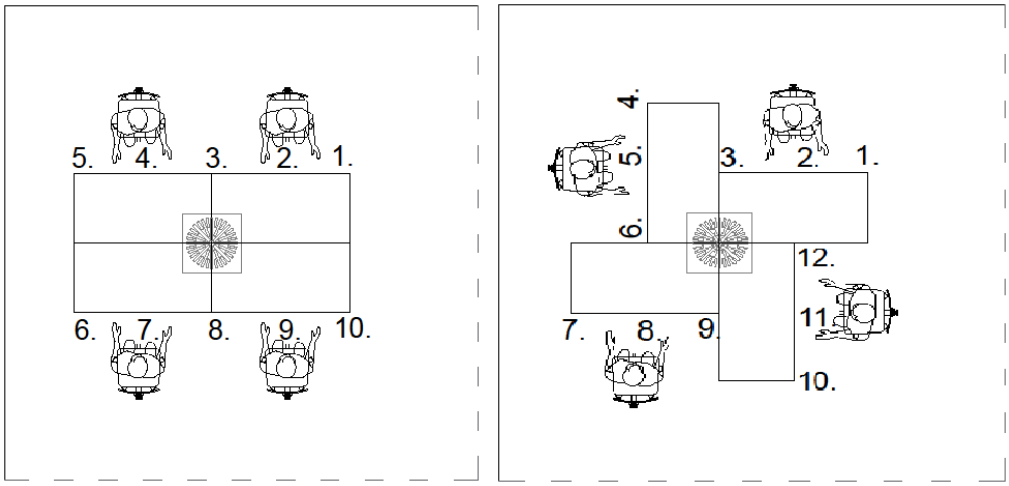

Figure 2. Workstation set-ups (**a**) island of four and measurement points (1–10), (**b**) flower and measurement points (1–12).

Ricciardi et al. in their article analyzed the thermal comfort in nine open plan offices with similar workstations as the examined set-ups with the same internal and external air temperatures [21]. With the right sitting distances set, high-impulse contaminant outflows (e.g., sneezing) are often protected with plexiglass sheets in office spaces. On that account, the effect of plexiglass placement for the selected table layouts was also examined. There are two effective ways to protect the occupants from developing contamination in the occupied zone. One is to keep a physical distance between the seated people, and the second one is to decrease the air mixing in the occupied zone [22].

The thermal comfort and indoor air quality of closed places are provided by the heating, ventilating, and air-conditioning (HVAC) systems.

Air ventilation in an office space can be divided into two major categories:

- displacement ventilation
- mixed ventilation

In mixed ventilation, the air is supplied near the ceiling or at the ceiling above the occupied zone and extracted mostly at the same level as the supplied air. (See Figure 3)

The manufacturers provide several types of inlet grilles also known as air diffusers.

Air diffuser (Figure 4): Supply air terminal device, usually placed in the ceiling, in a circular, square, or rectangular shape, and composed of divergent deflecting members.

The ceiling diffusers from Figure 4 were used in the experiment to serve as a reference for subsequent measurements. The most extensive series of measurements were performed with the diffuser "a" from Figure 4. With high induction the air in the occupied zone would swirl around in a spiraling pattern as shown in Figure 3, mixing the air in the occupied zone with the *primary air* flow (fresh air) sending the mixed air through the premises. Thus, the risk of infection is significantly higher [23]. Table 1 shows the maximum velocity (v_{max}), induction rate (i) and *primary air* percentage in the occupied zone (vol%) for several types of ceiling diffusers based on the manufacturing design programs.

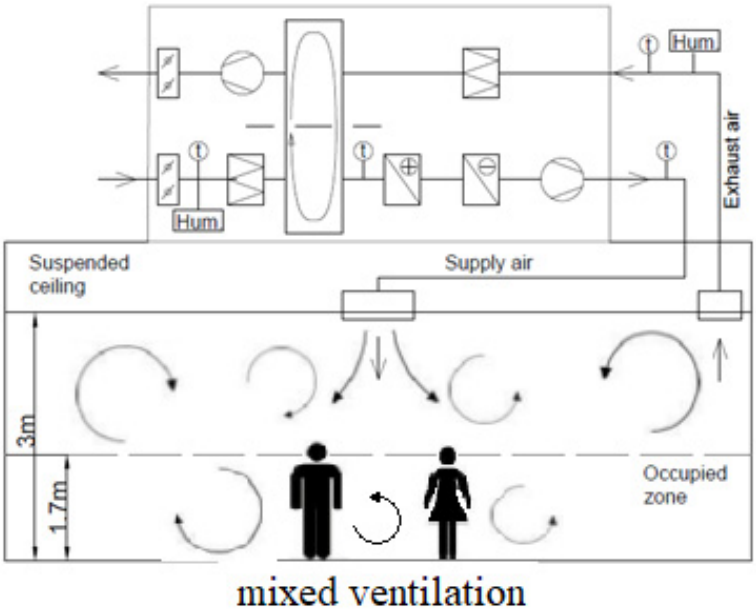

Figure 3. Swirls caused by the type of ventilation (schematic mode of the laboratory).

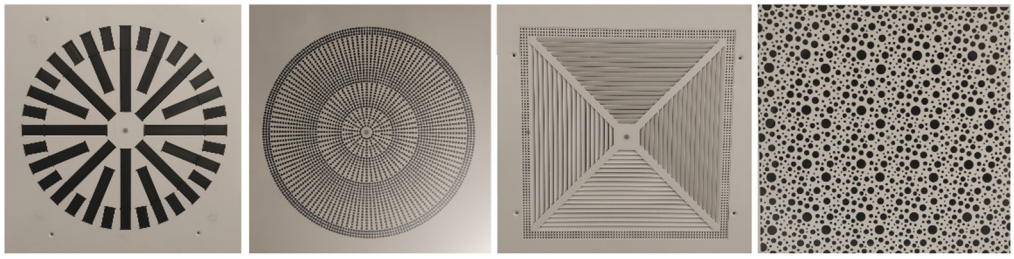

(**a**) (**b**) (**c**) (**d**)

Figure 4. Examined diffusers: (**a**) DQJA SR, (**b**) Pil-R-Z, (**c**) 4-DF, (**d**) Xarto-Q6.

Table 1. Air volume flow rate (500 [$m^3 \cdot h^{-1}$]), velocity, and induction number for different diffusers.

Name	v_{max} [$m \cdot s^{-1}$]	i v%
Schako-DQJA-SR	0.14	40.7 2.46
Schako-Pil-R-Z	0.15	24.5 4.08
Schako-4-DF	0.18	16.7 5.99
Trox-Xarto-Q6	0.12	-

Air velocity highly affects the thermal comfort in an office building which can lead to a high percentage of dissatisfied people [21].

Before starting the experiment, the air volume flow rate through the ceiling swirl diffuser was measured and then adjusted to 500 $m^3 \cdot h^{-1}$, which is an average flow rate for diffusers in offices. The mean air velocity, draught rate, and turbulence intensity were measured in the occupied zone at 1.1 m height, which is the head region for a sitting person.

2.2. Investigation Methods

The measurements have been carried out, in the Air-Ventilation and Air-Conditioning Laboratory. The primary function of the laboratory is to examine various air-conditioning and air ventilation systems.

– In the laboratory the following parameters were measured [Figure A1] during the investigation:
– temperature of *primary air* tp [°C]
– air temperature at the measured points in the occupied zone ta [°C]

– (1.1 m from the floor)
– air relative humidity RH [%]
– mean air velocity v [m·s^{-1}]

By means of these parameters the following values were calculated with Testo 400 instruments according to EN ISO 7730 [24]:

– Turbulence Intensity *TU* [%]:

$$TU = \frac{\sqrt{\frac{1}{n-1} \cdot \sum_{i=1}^{n} (xi - \overline{x})^2}}{\overline{v}} \cdot 100 \ [\%] \quad (1)$$

– Draught rating *DR* [%]:

$$DR = (34 - t_a)(v - 0.05)^{0.62}(0.37 \cdot v \cdot TU + 3.14) \ [\%] \quad (2)$$

These parameters are not enough to value the *primary air* rate in the occupied zone, therefore, a numerical model was used to simulate the airflow in this area and determined the:

– Induction ratio *i* [-]

The amount of mixing caused by the airflow entering the occupied zone can be characterized by the induction rate.

Several diffuser manufacturers in their technical documentation define the fundamentals of air distribution and essential properties of diffusers (SCHAKO, Air Breeze, AirVent, Trox: Neukirchen-Vluyn, Germany).

$$i = \frac{total\ air}{primary\ air} \quad (3)$$

$$i = \frac{primary\ air + secondary\ air}{primary\ air} \quad (4)$$

– *primary air*: the air coming directly from the diffuser
– *secondary air*: the room air which is picked up and carried along by the *primary air*
– *total air*: the entire stream is composed of a mixture of primary and *secondary air*

Induction ratio (*i*), is defined as the ratio of *total air* to *primary air*.

2.3. Numerical Model

The induction rate of the airflow around the seated person, as well as the secondary airflow induced by the primary airflow, were examined using a computational fluid dynamic simulation. In the numerical model, the actual laboratory was digitally created where the measurements happen. The main purpose was to showcase a simulation-driven design process, where firstly a model was created that resembles an actual laboratory measurement.

To reduce the computational demand for the simulation, localized mesh refinement was applied in the domain (see Figure 5a). In general, 120 mm large hexahedrons were used in the room. Two 15 mm mesh refinement was applied, one was a 600 mm diameter column between the table and the inflow diffuser, and one was a table enclosure where 400 m was left on the topside and 50 mm from the rest. On the top side of the table, larger refinement was needed since that is the relevant volume and in addition, the velocity measurements were taken from here. This diffuser was simplified to an N-point air supply opening model (see Figure 5b) [25], where the fluid cross-section area and the longer width of the diffuser were matched. This allowed the coarser mesh to be applied where the meshing should have been finer. Attributable to the time-averaged velocity values Reynolds averaged numerical simulations were used in the cases. During the development of the flow model, the time dependency was examined, and a high similarity showed between the time-dependent and pseudo-steady models. Thus, in the paper, only the pseudo-transient results are presented. Usually for diffusers and jet flows only two-equation k-epsilon turbulence

models are favored and, in many cases, Refs. [26–29] are examined with good correlations. However, from the table flow, separation is excepted which could cause the turbulence around the measured area and due to complex flow, the k-omega SST model was used. The k-omega SST models are rarely used, however, Mao et al. [30] work showed promising results predicting indoor airflow, this was also summarized in the work of Zhai et al. [31] work. It must be mentioned that in some thermal models the k-omega model's weakness can be that it overpredicts the heat flow as Liu et al. reported [26], yet the showcased model is isothermal. Since large swirling flows were modeled, a pressure and velocity coupling solver was used; for pressure calculation the PRESTO! scheme and for momentum, the turbulent kinetic energy and turbulent dissipation rate solution with a second-order upwind scheme was applied. For the simulations, Ansys2021R2 was used. To evaluate the simplification of the diffuser geometry, two sets of simulations were made, one where the actual diffuser geometries (provided by the manufacturers) and the simplified N-point air supply model version of them were applied. For these simulations, the domain was only a 0.5 m radius and column. The mesh from the geometries was made from 5–20 mm cell size mesh. For the evaluation, contour plots of velocity magnitudes were used, and values were mapped at x-y and z-y cross-sections and presented in Figure 6.

Red dashed lines represent the detailed diffuser geometry values, and black is the simplified N-point diffuser geometry. Figure 6a,b shows that two sets of contours are overlapping each other. The difference between the two types of discretization can be showcased in a boxplot (Figure 6c). One can see that the median values are close to each other at both the y-x and y-z planes. On the y-x plane, a smaller deviation can be seen, which can be owing to the fins of the diffuser while the absence of the fins leads to smaller deviation on the y-z plane for the coarser/simplified case. The difference between the coarse and fine mesh due to the low magnitude of velocity is acceptable. The error between the two mesh is not calculated since the different discretization density does not allow for calculating the exact error. In further simulations, only the simplified versions of the diffusers were used. A classic mesh dependency study was not made, however, mesh refinement at certain zones decreased the difference between the modeled and measured velocities.

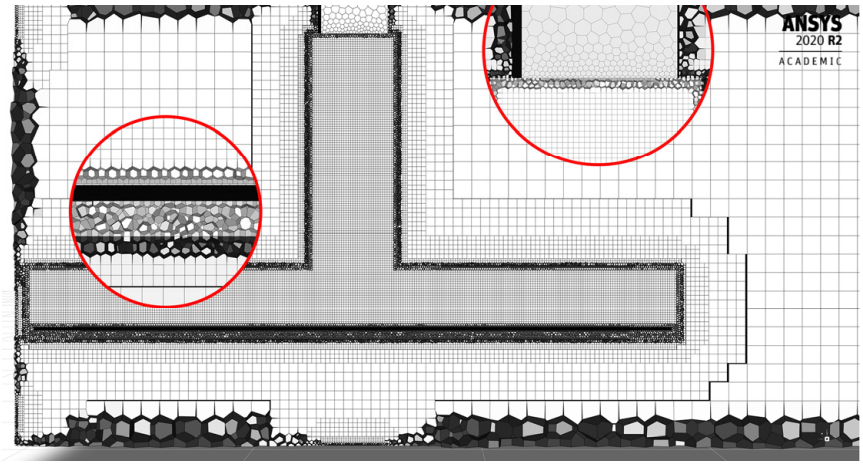

(**a**)

Figure 5. *Cont.*

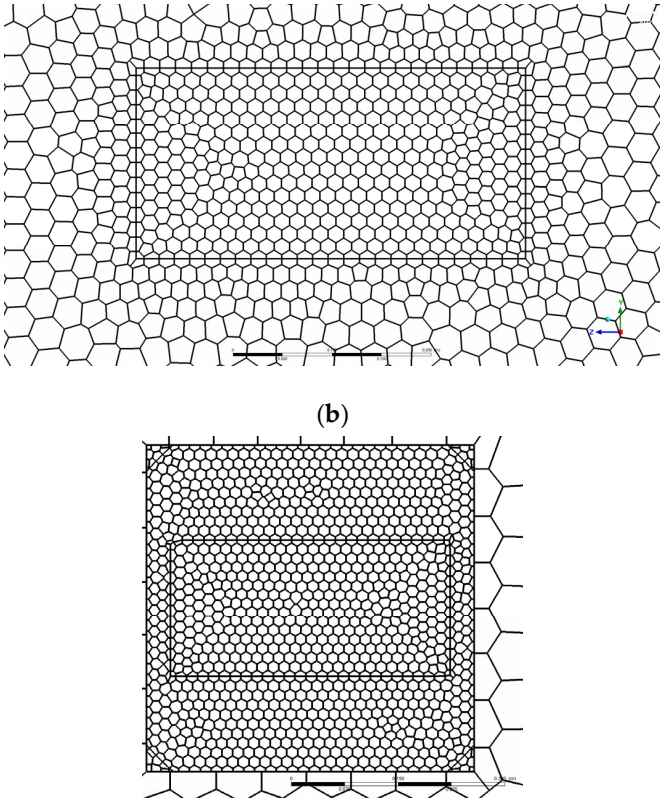

Figure 5. Mesh refinement zones (**a**), top view of the inlet diffuser mesh (**b**), side view of the exhaust diffuser (**c**).

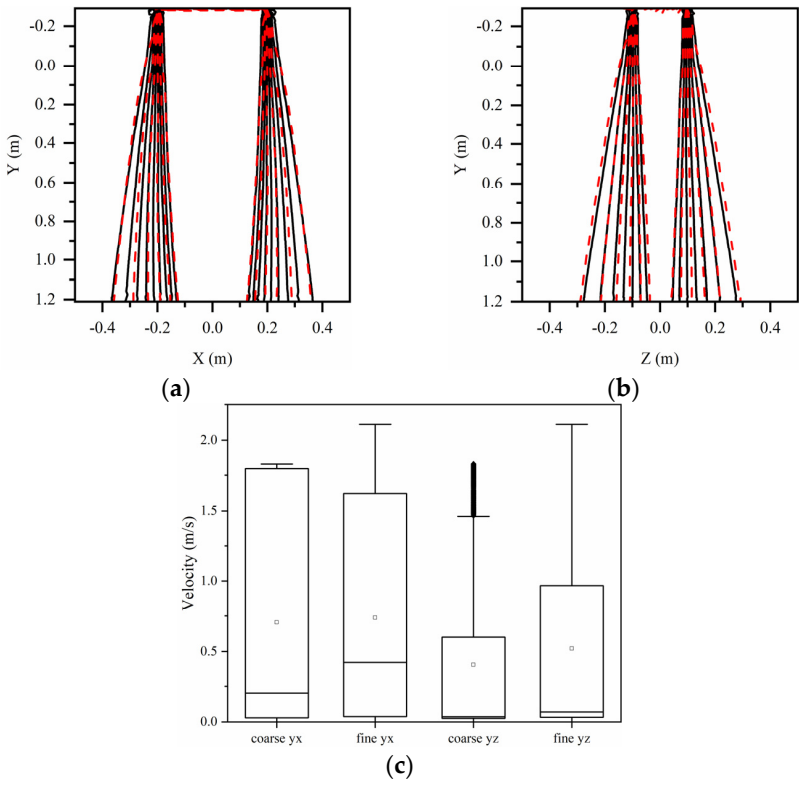

Figure 6. Velocity mapping for y-x (**a**) and y-z (**b**) planes and (**c**) boxplot of velocities.

3. Developed Air Ventilation System Element (Air-Jet Control Box)

Most office spaces are equipped with mixed ventilation, which leads to higher contamination concentration in the occupied zone. To lower the risk of transmission of viruses, the induction rate of the diffusers needs to be decreased which leads to more evenly distributed *primary air* in the occupied zone. There are two effective ways to protect the occupants from developing contamination in the occupied zone. One is to keep a physical distance between the seated people, and the second one is to decrease the air mixing in the occupied zone. Acknowledging this, investigations have been conducted to find which air supply equipment has a low induction rate. During the study, it was concluded that a more advantageous flow pattern can be achieved with the vent grilles as can be seen in Table 2 based on the manufacturer's design software (Schako Luft).

Table 2. Induction rates of swirl diffuser compared to a grill.

Air Supply Equipment Parameters	SCHAKO-DQJA-SR Swirl Diffuser [Figure A2] i	SCHAKO-KG215-415 Grill i
500 $m^3 \cdot h^{-1}$; isotherm	40.7	3.8
500 $m^3 \cdot h^{-1}$; cooling (ΔT = 5 K)	37.8	2.7

To be able to change the airflow pattern on existing ceiling diffusers and examine the effect of low induction rate in the occupied zone, an attachment to ceiling swirl diffusers on the supply air installation was developed, referred to as "air-jet control box" as can be seen in Figure 7.

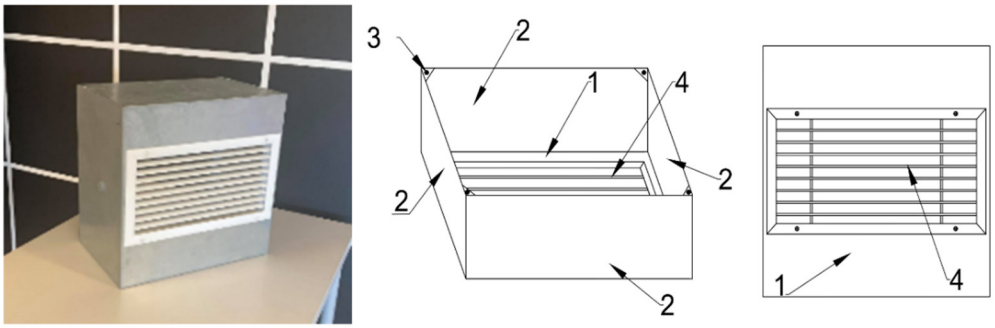

Figure 7. Developed air-jet control box. 1. Front panel; 2. Side panel; 3. Magnetic button; 4. Air grille.

This attachment has similar characteristics to a box, except the top side is open, and the bottom side has an air vent grill mounted on it. The goal was to create something that will reduce the high induction rate produced by the mixed ventilation air diffuser. With this attachment the induction rate is lower; therefore, the primary airflow will swirl considerably less. The air-jet control box was designed to fit on 600 mm × 600 mm diffusers. It is fixed with magnets, therefore, it can be installed and removed easily without making any damage and does not require any expertise. The primary airflow entering the air-jet control box swirls and leaves with a flow pattern corresponding to the built-in air grille (Schako-KG215-415). The air-jet control box was mounted on the Schako-DQJA-SR supply diffuser, and it was set to deliver an airflow of 500 $m^3 \cdot h^{-1}$, so the changes in the flow patterns and the comfort parameters of the seating position could be observed. With the help of the air-jet control box attachment, the pattern of the primary airflow can be changed without having to make a permanent change to the existing ventilation system. The attachment did not cause a significant reduction in air volume, its resistance is low (measured pressure drop: 1.8 Pa; 500 $m^3 \cdot h^{-1}$), so it can be applied to the endpoints of an extensive ventilation system without the need for hydraulic adjustment.

If it is required, the direction of the airflow can also be controlled by adjusting the vent grills' position. The effect of the induction rates on different diffusers and vent grills in an

office environment was measured and simulated. In Figure 8 the experimental airflow can be seen, compared with the modeled airflow. The Reynolds-averaged method simplifies the velocity distribution; thus, it only gives a rough estimate of the flow profile. For a more detailed view, the Q-criterion was also added to depict the vortices that were generated by the inlet flow. Particle Image velocimetry can be also used to depict the velocity profiles [32], yet a numerical approach was preferred for further optimization purposes.

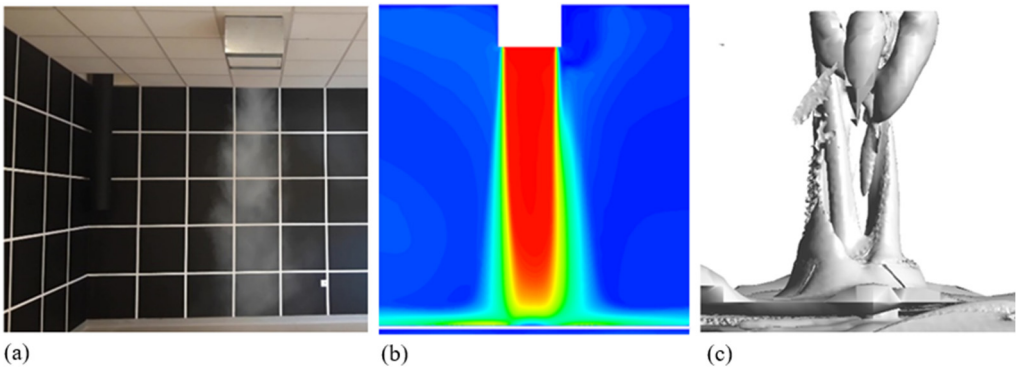

Figure 8. Experimental (**a**), modelled velocity (**b**) and Q-criterion (**c**) diffuser inflow.

4. Model Verification

In the computational domain, the only relevant surface that could alter the velocity magnitudes is the table surface. This can be attributed to the examination area being purposely placed away from the wall. Above the table, the y^+ deviated between 11 and 27, based on the model verification, it was considered to be acceptable. Experimental and modeled results were compared both visually and numerically. During the measurement, photos were taken, and the shape of the flow was compared. In Figure 8a a photo taken during the experiment, in Figure 8b, the control case velocity plot and in Figure 8c the Q-criterion = 0.012 s^{-2} can be seen. Based on the visual comparison of Figure 8a,b, one can see that the smaller vortices are disregarded due to the k-omega SST model, in addition, it leads to the velocity cone becoming smaller than the actual smoke cone. The asymmetric flow shape that is depicted in Figure 8a can be visualized by the Q-criterion. Larger than 0.012 s^{-2} values were chosen since this value is low enough to show the predicted inflow cone shape while it is large enough to filter the small vortices that could interfere in the visualization. At certain points, velocities were measured which served as a basis for the numerical comparison. In Figure 9, experimental and modeled velocities at the measured positions for "flower" (a), and "island of four" (b) are plotted. For indoor ventilation, all the cases showed low magnitudes, thus slight 0.02 ms^{-1} deviations would mean a considerable magnitude of errors.

The applied simulation model in the "flower" arrangement (a) overpredicted while in the "island of four" arrangement (b) underpredicted the velocity values. The difference between the measured and modeled values can be attributed to the complex low magnitude flow Figure 9. The highest underprediction occurred at the fifth and sixth position on the "flower" arrangement, the underprediction can be attributed to the peaking measurement values. Both peaking deviations were examined multiple times and they occurred repeatedly. Based on both numerical and visual comparison it is assumed that the applied numerical calculation method can represent the actual indoor flow.

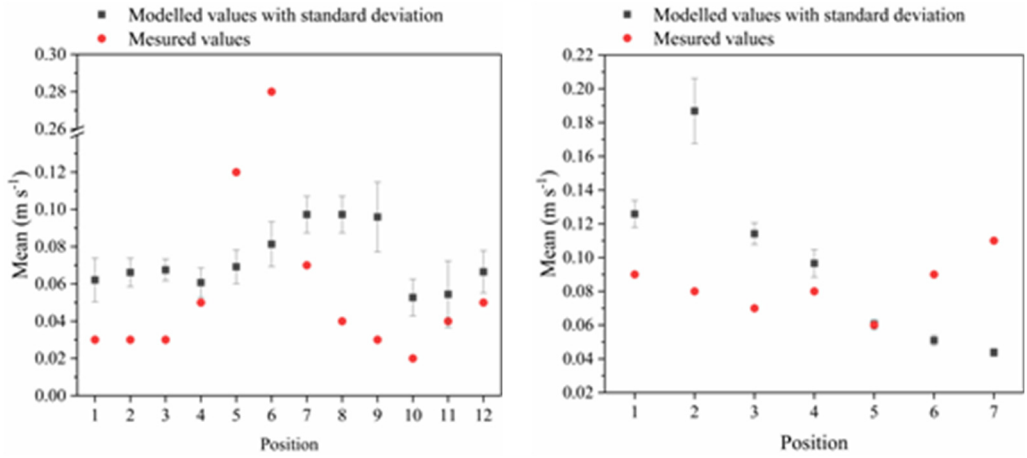

(**a**) (**b**)

Figure 9. Measured and modelled air velocities at the measured positions for (**a**) "flower", (**b**) "island of four".

5. Results and Discussion of Measurement for the Air-Jet Control Box

During the measurements, the comfort parameters experienced in the sitting position for the previously selected desk layouts were examined, with and without plexiglass sheets.

From Figures 10–13, it can be seen that the *primary air* stream mixes less *secondary air* when using the air-jet control box. Therefore, the surface of the desk is reached in a more concentrated manner by the primary airflow, hence the condition of the air in the occupied zone in the sitting positions is similar to the air supplied by the HVAC unit. Along the surface of the desks, the airflow spreads and reaches the position of the seated person. The same series of measurements have been performed using an air-jet control box and compared the results of measurements with each other. In this case too, in Tables 3 and 4, the results from the three minutes average of the measurements were presented according to ISO 7726 [33].

(**a**) (**b**)

Figure 10. Air Flow pattern without (**a**) and with the air-jet control box (**b**) examined with the "Island of four" setup.

(**a**) (**b**)

Figure 11. Air Flow pattern without (**a**) and with the air-jet control box (**b**) including plexiglass examined with the "Island of four" setup.

(**a**) (**b**)

Figure 12. Air Flow pattern without (**a**) and with the air-jet control box (**b**) examined with the "Flower" setup.

(**a**) (**b**)

Figure 13. Air Flow pattern without (**a**) and with the air-jet control box (**b**) including plexiglass examined with the "Flower" setup.

Table 3. Airflow status indicators at the Island of four setup.

Island of Four Layout (ta: 23.9–24.4 °C)												
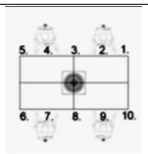	Empty Desktop						Desktop with Plexiglass					
	DQJA SR			Air-Jet Control Box			DQJA SR			Air-Jet Control Box		
Measure Points	V [m·s^{-1}]	TU [%]	DR [%]	v [m·s^{-1}]	TU [%]	DR [%]	v [m·s^{-1}]	TU [%]	DR [%]	v [m·s^{-1}]	TU [%]	DR [%]
2	0.03	66	0	0.09	58	7	0.03	67	0	0.14	51	13
4	0.10	54	7	0.12	45	10	0.07	90	4	0.09	47	7
7	0.04	68	0	0.07	72	5	0.08	55	5	0.07	54	3
9	0.02	79	0	0.08	56	6	0.02	66	0	0.07	70	5

Table 4. Airflow status indicators at the Flower setup.

Flower Layout (ta: 23.9–24.4 °C)												
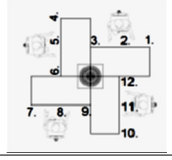	Empty Desktop						Desktop with Plexiglass					
	DQJA SR			Air-Jet Control Box			DQJA SR			Air-Jet Control Box		
Measure Points	v [m·s^{-1}]	TU [%]	DR [%]	v [m·s^{-1}]	TU [%]	DR [%]	v [m·s^{-1}]	TU [%]	DR [%]	v [m·s^{-1}]	TU [%]	DR [%]
2	0.03	66	0	0.16	44	15	0.02	63	0	0.07	72	5
5	0.12	85	11	0.09	57	6	0.06	90	3	0.06	62	2
8	0.04	68	0	0.06	61	2	0.08	47	5	0.11	70	9
11	0.04	70	0	0.06	79	3	0.02	61	0	0.06	80	2

According to Table 3, by using the air-jet control box, the flow status indicators in the sitting position remain at an adequate comfort level [Table A1], [34].

According to Table 4, by using the air-jet control box, the flow status indicators in the sitting position remain at an adequate comfort level [Table A1], [34] and even a slight improvement in flow status indicators can be observed. Based on the measurement results and by analyzing Figures 10–13, it can be concluded that when using the air-jet control box, the induction rates were reduced, and the comfort parameters did not change significantly in the sitting position. By using the air-jet control box, ensuring the appropriate distance, and by using the plexiglass sheet, a micro-environment can be created for the workers in which the comfort conditions do not differ significantly compared to the application of the traditional ventilation system; however, the spread of contaminants from worker to worker, is significantly reduced.

Induction Rate in the Occupied Zone Based on Simulations

In the numerical models, and the volume fractions of the *primary air* and *secondary air* were looked up in the zone where mesh refinement was applied. The *primary air* volume concentration for the island of four is 21.4 vol% and for the flower arrangement is 18.3 vol%, respectively. With the air-jet control box, a considerable amount of fresh air flowed into the relevant area, yet it must also notice that the secondary flow had a low speed which is favorable.

The induction rate from the numerical model results was examined. The volume percentage was converted from the results to induction rate, which in the case of the "island of four" setup is 4.67 and in the case of the "flower" setup is 5.46. Both values are exceptionally good news as it verifies the results of the manufacturer's design program and the nomograms for sizing (see Table 2). These results prove that the induction rate significantly decreased while using the air-jet control box compared to the conventional mixing ventilation.

Awbi demonstrated on various kinds of jet systems that if the induction rate is reduced, better air quality is achieved in the occupied zone [35].

The inflow with the air-jet control box increased the kinetic energy of the flow and most of it reached the tables where it was scattered in every direction. The examined cases where the air-jet control box was used were favorable as the occupied zone of the person sitting by the desks is continuously under a fresh air supply with a lower induction rate than at mixed ventilation Table 5.

Table 5. Induction rate and *primary air* percentage.

Air Supply Equipment	Type of Office Layout	Based on Estimation	Estimated Value of Induction Rate	Volume Percentage of *Primary Air*
SCHAKO-DQJA-SR swirl diffuser	not defined	Designer software of manufacturer	40.7	2.46
Air-Jet Control Box	Island of four	Simulation	4.67	21.41
Air-Jet Control Box	Flower	Simulation	5.46	18.32

6. Conclusions

It is necessary to ensure the protection of office workers returning to office buildings to reduce the spread of contaminants, bacteria, and viruses and increase the fresh air rate in the occupied zone. With the right design of the office layouts, a suitable distance can be set between the workstations which can protect the workers against larger particle size contaminants. Besides the distance, the use of a plexiglass sheet provides additional protection against high impulse contaminants. The commonly used ventilation systems in the offices can only achieve the desired comfort parameters of air with significant mixing. The degree of mixing can be characterized by the induction rate.

In this article, an innovative design approach was elaborated where all workstations are placed right under the diffusers. The effects of the worktops and barriers to the air velocity, turbulence grade and draught rate were analyzed.

1. One of the most common ventilation types in offices is mixed ventilation. In this ventilation mode, the infection probability is high because of the properties of the airflow.
2. At the UD, a new air-ventilation service element was developed and named as "air-jet control box". This attachment allows for modifying the properties of the ceiling diffusers used in office buildings to suit the temporary conditions. Such properties are the airflow control, air velocity, temperature, and induction rate in the occupied zone.
3. The aim was to supply as much fresh air as possible in the occupied zone with the air velocity allowed by the standards. The equipment did not cause a significant reduction in air volume, its resistance is low, therefore, it does not lead to higher energy consumption.
4. It was shown that when using the air-jet control box, the induction rate was reduced, and the comfort parameters did not change significantly in the sitting position.
5. Based on design software, the fresh air ratio for the standard ceiling swirl diffuser is 2.46 v% (volume percentage). Numerical models show that the fresh air ratio with the air-jet control box for the two different desk arrangements was 18.3 v% (flower layout) and 21.4 v% (island of four), respectively.

Thus, the degree of contamination in the microenvironment of the worker is improved and the comfort parameters remain suitable. Therefore, it is possible to upsize the staff in office buildings while providing a safe environment in the occupied zone of a sitting person.

7. Future Plans and Different Fields of Application

A future research perspective is to analyze and modify the air jet control box geometry size and weight to simplify the connection to diffusers see Figure 14.

Figure 14. Upgraded air jet control box.

In some situations, the modification of the office plans, office area, function of the room, activity in the room, and workstation layouts can cause thermal discomfort issues (draught rate) which could be solved by using the air jet control box.

A concept was elaborated to smarten up the element by placing integrated sensors inside to monitor the air quality and collect all data and report regularly, plus if needed, alert the occupant via the internet.

Author Contributions: Conceptualization, I.C., A.K. and S.S.; Methodology, I.C., A.K. and S.S.; Software, I.C., F.S., A.K. and S.S.; Validation, I.C., F.S., A.K. and S.S.; Formal Analysis, I.C., F.S., A.K. and S.S.; Investigation, I.C., F.S., A.K. and S.S.; Resources, I.C., F.S., A.K. and S.S.; Data Curation, I.C., F.S., A.K. and S.S.; Writing—Original Draft Preparation, I.C., F.S., A.K. and S.S.; Writing—Review & Editing, I.C., A.K. and S.S.; Visualization, I.C., F.S., A.K. and S.S.; Supervision, I.C. All authors have read and agreed to the published version of the manuscript.

Funding: This research was funded by the Thematic Excellence Programme (TKP2020-IKA-04) of the Ministry for Innovation and Technology in Hungary.

Institutional Review Board Statement: Not applicable.

Informed Consent Statement: Not applicable.

Data Availability Statement: Not applicable.

Conflicts of Interest: The authors declare no conflict of interest.

Nomenclature

UD	University of Debrecen
tp	temperature of *primary air* [°C]
ta	air temperature at the measured points in the occupied zone [°C]
RH	air Relative Humidity [%]
v	mean air velocity [m·s^{-1}]
TU	Turbulence Intensity [%]
n	number of measurements
xi	measured value
$\bar{\mathbf{x}}$	average of measured value
DR	Draught rate [%]
i	Induction ratio [-]
vol%	volume percentage [%]
DQJA-SR	swirl diffuser type by Schako Vertriebs GmbH
Pil-R-Z	impulse diffuser type by Schako Vertriebs GmbH
4-DF	ceiling diffuser type by Schako Vertriebs GmbH
Xarto-Q6	swirl diffuser type by TROX GmbH
KG-215-415	air grill type by Schako Vertriebs GmbH

Appendix A

Instruments

During the experiments, the following calibrated instruments were used (see Figure A1):
TESTO 400 instrument.

Turbulence intensity probe structure sensor, guard, probe shaft, handle, and cable:

According to the calibration certificate, the uncertainty of measured velocities is 0.02 m·s^{-1}, coverage factor k = 2.95% confidence. The instrument calculates the turbulence intensity and draught rate based on ISO 7730 [24].

Air temperature probe structure sensor, guard, probe shaft, handle, and cable:

According to the calibration certificate, the uncertainty of measured air temperatures is 0.03 °C, coverage factor k = 2.95% confidence.

For the smoke test, a Martin Magnum 650 smoke machine was used.

Figure A1. Instruments.

Appendix B

Induction Rate: SCHAKO DQJA SR Swirl Diffuser

Figure A2. Air Flow pattern.

Appendix C

Thermal Comfort Requirements

The thermal comfort requirements needed in enclosed spaces are contained in the standards MSZ CR 1752: 2000 (see Table A1) [34].

Table A1. Comfort categories according to standards MSZ CR 1752: [34].

Comfort Category	Operative Temperature [°C]		Average Air Velocity [m·s^{-1}]	
	Summer (Cooling)	Winter (Heating)	Summer (Cooling)	Winter (Heating)
A	24.5 ± 1.0	22.0 ± 1.0	0.18	0.15
B	24.5 ± 1.5	22.0 ± 2.0	0.22	0.18
C	24.5 ± 2.5	22.0 ± 3.0	0.25	0.21

References

1. Antoniadou, P.; Papadopoulos, A.M. Occupants' thermal comfort: State of the art and the prospects of personalized assessment in office buildings. *Energy Build.* **2017**, *153*, 136–149. [CrossRef]
2. Pérez-Lombard, L.; Ortiz, J.; Pout, C. A review on buildings energy consumption information. *Energy Build.* **2008**, *40*, 394–398. [CrossRef]
3. WHO. Coronavirus Disease (COVID-19): How Is It Transmitted? Available online: www.who.int/news-room/questions-and-answers/item/coronavirus-disease-covid-19-how-is-it-transmitted (accessed on 24 February 2022).
4. ASHRAE. Ashrae Position Document on Infectious Aerosols. Available online: www.ashrae.org/file%20library/about/position%20documents/pd_infectiousaerosols_2020.pdf (accessed on 24 February 2022).
5. REHVA. Rehva COVID-19 Guidance. Available online: http://www.rehva.eu/fileadmin/user_upload/REHVA_COVID-19_guidance_document_ver2_20200403_1.pdf (accessed on 24 February 2022).
6. Cao, S.-J.; Ren, C. Ventilation control strategy using low-dimensional linear ventilation models and artificial neural network. *Build. Environ.* **2018**, *144*, 316–333. [CrossRef]
7. Luo, M.; Cao, B.; Damiens, J.; Lin, B.; Zhu, Y. Evaluating thermal comfort in mixed-mode buildings: A field study in a subtropical climate. *Build. Environ.* **2015**, *88*, 46–54. [CrossRef]
8. Hummelgaard, J.; Juhl, P.; Sæbjörnsson, K.; Clausen, G.; Toftum, J.; Langkilde, G. Indoor air quality and occupant satisfaction in five mechanically and four naturally ventilated open-plan office buildings. *Build. Environ.* **2007**, *42*, 4051–4058. [CrossRef]
9. Nguyen, A.T.; Singh, M.K.; Reiter, S. An adaptive thermal comfort model for hot humid South-East Asia. *Build. Environ.* **2012**, *56*, 291–300. [CrossRef]
10. Damiati, S.A.; Zaki, S.A.; Rijal, H.B.; Wonorahardjo, S. Field study on adaptive thermal comfort in office buildings in Malaysia, Indonesia, Singapore, and Japan during hot and humid season. *Build. Environ.* **2016**, *109*, 208–223. [CrossRef]
11. Pereira, P.F.; Ramos, N.M.M. The impact of mechanical ventilation operation strategies on indoor CO_2 concentration and air exchange rates in residential buildings. *Indoor Built Environ.* **2021**, *30*, 1516–1530. [CrossRef]
12. Persily, A.K. The relationship between indoor air quality and carbon dioxide. In Proceedings of the 7th Indoor Air Quality and Climate, Nagoya, Japan, 21–26 July 1996; pp. 961–966.

13. Kalmár, T.; Kalmár, F. Investigation of natural aeration in home offices during the heating season—Case study. *J. Build. Eng.* **2020**, *35*, 102052. [CrossRef]
14. Cardoso, V.E.M.; Pereira, P.F.; Ramos, N.M.M.; Almeida, R.M.S.F. The Impacts of Air Leakage Paths and Airtightness Levels on Air Change Rates. *Buildings* **2020**, *10*, 55. [CrossRef]
15. Junghans, L.; Widerin, P. Thermal comfort and indoor air quality of the "Concept 22/26", a new high performance building standard. *Energy Build.* **2017**, *149*, 114–122. [CrossRef]
16. Valančius, R.; Jurelionis, A. Influence of indoor air temperature variation on office work performance. *J. Environ. Eng. Landsc. Manag.* **2012**, *21*, 19–25. [CrossRef]
17. Kang, S.; Ou, D.; Mak, C.M. The impact of indoor environmental quality on work productivity in university open-plan research offices. *Build. Environ.* **2017**, *124*, 78–89. [CrossRef]
18. Szczepanik-Scislo, N.; Schnotale, J. An Air Terminal Device with a Changing Geometry to Improve Indoor Air Quality for VAV Ventilation Systems. *Energies* **2020**, *13*, 4947. [CrossRef]
19. Szczepanik-Scislo, N.; Scislo, L. Comparison of CFD and Multizone Modeling from Contaminant Migration from a Household Gas Furnace. *Atmosphere* **2021**, *12*, 79. [CrossRef]
20. Liu, L.; Li, Y.; Nielsen, P.V.; Wei, J.; Jensen, R.L. Short-range airborne transmission of expiratory droplets between two people. *Indoor Air* **2016**, *27*, 452–462. [CrossRef]
21. Ricciardi, P.; Buratti, C. Thermal comfort in open plan offices in northern Italy: An adaptive approach. *Build. Environ.* **2012**, *56*, 314–320. [CrossRef]
22. Sun, C.; Zhai, Z. The efficacy of social distance and ventilation effectiveness in preventing COVID-19 transmission. *Sustain. Cities Soc.* **2020**, *62*, 102390. [CrossRef]
23. Ren, C.; Zhu, H.-C.; Cao, S.-J. Ventilation Strategies for Mitigation of Infection Disease Transmission in an Indoor Environment: A Case Study in Office. *Buildings* **2022**, *12*, 180. [CrossRef]
24. *ISO 7730-1994*; Moderate Thermal Environments-Determination of the PMV and PPD Indices and Specification of the Conditions for Thermal Comfort. International Organization for Standardization: Geneva, Switzerland, 1994.
25. Zhao, B.; Li, X.; Yan, Q. A simplified system for indoor airflow simulation. *Build. Environ.* **2003**, *38*, 543–552. [CrossRef]
26. Liu, J.; Zhu, S.; Kim, M.K.; Srebric, J. A Review of CFD Analysis Methods for Personalized Ventilation (PV) in Indoor Built Environments. *Sustainability* **2019**, *11*, 4166. [CrossRef]
27. Szodrai, F.; Kalmár, F. Simulation of Temperature Distribution on the Face Skin in Case of Advanced Personalized Ventilation System. *Energies* **2019**, *12*, 1185. [CrossRef]
28. Lin, H.-H. Improvement of Human Thermal Comfort by Optimizing the Airflow Induced by a Ceiling Fan. *Sustainability* **2019**, *11*, 3370. [CrossRef]
29. Posner, J.; Buchanan, C.; Dunn-Rankin, D. Measurement and prediction of indoor air flow in a model room. *Energy Build.* **2002**, *35*, 515–526. [CrossRef]
30. Mao, N.; Song, M.; Deng, S.S.; Pan, D.; Chen, S. Experimental and numerical study on air flow and moisture transport in sleeping environments with a task/ambient air conditioning (TAC) system. *Energy Build.* **2016**, *133*, 596–604. [CrossRef]
31. Zhai, Z.J.; Zhang, Z.; Zhang, W.; Chen, Q.Y. Evaluation of Various Turbulence Models in Predicting Airflow and Turbulence in Enclosed Environments by CFD: Part 1—Summary of Prevalent Turbulence Models. *HVAC&R Res.* **2007**, *13*, 853–870. Available online: https://engineering.purdue.edu/~{}yanchen/paper/2007-8.pdf (accessed on 8 February 2022).
32. Szczepanik-Scislo, N.; Antonowicz, A.; Scislo, L. PIV measurement and CFD simulations of an air terminal device with a dynamically adapting geometry. *SN Appl. Sci.* **2019**, *1*, 370. [CrossRef]
33. *ISO 7726-1998*; Ergonomics of the Thermal Environment—Instruments for Measuring Physical Quantities. International Organization for Standardization: Geneva, Switzerland, 1998.
34. *MSZ CR 1752:2000*; Ventilation for Buildings. Hungarian Standard Commitment: Budapest, Hungary, 2000.
35. Ganguly, S.; Tan, L.; Date, A.; Kumar, M.S.M. Effect of Heat Loss in a Geothermal Reservoir. *Energy Procedia* **2017**, *110*, 77–82. [CrossRef]